

See discussions, stats, and author profiles for this publication at: <https://www.researchgate.net/publication/30472982>

Femtosecond Twisting and Coherent Vibrational Motion in the Excited State of Tetraphenylethylene

ARTICLE *in* THE JOURNAL OF PHYSICAL CHEMISTRY · JUNE 1995

Impact Factor: 2.78 · DOI: 10.1021/j100022a006 · Source: OAI

CITATIONS

35

READS

24

3 AUTHORS, INCLUDING:



[Douwe A. Wiersma](#)

University of Groningen

203 PUBLICATIONS 7,309 CITATIONS

SEE PROFILE

Femtosecond Twisting and Coherent Vibrational Motion in the Excited State of Tetraphenylethylene

Egbert Lenderink, Koos Duppen, and Douwe A. Wiersma*

Ultrafast Laser and Spectroscopy Laboratory, Department of Chemical Physics/Materials Science Centre, University of Groningen, Nijenborgh 4, 9747 AG Groningen, The Netherlands

Received: December 9, 1994; In Final Form: March 17, 1995*

The initial dynamics after excitation to the S_1 state of tetraphenylethylene is studied using femtosecond pump–probe spectroscopy. From the rapid spectral changes during the first few hundred femtoseconds, we conclude that a fast ethylenic twisting motion occurs in the excited state within this time period. We observe a coherent oscillation, building up during the twist and then decaying rapidly, which we ascribe to the concerted response of the phenyl rings to the release of steric strain. The subsequent full geometric relaxation of the distorted molecule is hindered by collisions with the solvent molecules and takes several picoseconds, dependent on solvent viscosity. The motions involved in this relaxation process govern the formation of a charge-separated (cs) state and the equilibrium that is established between this cs state and the nonpolar excited state.

1. Introduction

Over the past decade, femtosecond spectroscopy has been developed and used as a tool to study the dynamics of chemical reactions.¹ Because of their large frequency bandwidth and short time duration, femtosecond laser pulses are able to excite a molecule to a coherent superposition of a large number of vibrational states. Thus, a moving wave packet can be formed in the excited state of a photochemical reactant.² In some photochemical systems, it was demonstrated that a femtosecond laser initiated reaction can also result in a coherent vibrational wave packet in the reaction product,³ even in the condensed phase.^{4–6}

Although the presence of vibrational coherence in photochemical systems has been firmly established, many questions remain. For instance, it is still an open question under what conditions coherence can be excited in the products or transferred from reactants to products. A second question is whether any observed excited state vibrational coherence is really relevant to the reaction pathway. It could take place in some “uninteresting” vibrational mode that is coupled to the excitation, but does not take part in the actual product formation. The latter question is very difficult to answer for complicated systems, such as biomolecular complexes.⁷

From theoretical studies,⁸ there are clear indications that coherent motion is an important factor in chemical reactivity, especially in cases where there is no substantial barrier present along the reaction coordinate. A full understanding of coherent effects in chemistry is necessary if one wants to describe these reactions properly. For instance, the familiar notion of a rate constant becomes meaningless if coherent motion takes place along the reaction coordinate on the time scale of the reaction.

A class of reactions in which many examples of barrierless processes are found is the photoassisted *cis*–*trans* isomerization, occurring through a 90° twist of the olefinic bond in the lowest singlet excited state.⁹ The most simple example is the ethylene molecule, which has been the subject of several theoretical studies.¹⁰ Many time-resolved experimental studies have been devoted to the isomerization of the stilbenes (*cis*- and *trans*-1,2-diphenylethylene).¹¹ These reactions have attracted attention

as models for olefinic isomerizations in biological systems. The process of vision, for instance, is triggered by the barrierless *cis*- to *trans* isomerization of an olefinic bond in the chromophore of the visual pigment protein rhodopsin.^{6,12} Here, as in *cis*-stilbene, the excited-state twist is (nearly) barrierless, and the time needed to reach the 90° twisted conformation is on the order of a few hundred femtoseconds. It has recently been observed that the process of vision also involves coherent product vibrations along the isomerization coordinate.⁶

In this paper, we will focus on the excited state twisting of tetraphenylethylene (TPE; $[C_6H_5]_2C=C[C_6H_5]_2$) in solution. From the observed dual fluorescence,¹³ it was inferred that the 90° excited-state twist of the central ethylenic bond of TPE takes place in 5–15 ps. A transient with the same lifetime was found around 450–500 nm and was assigned to the “planar” excited state; a long-lived (nanoseconds) component was observed around 550 nm and assigned to the twisted conformer. The large frequency difference between the excitation wavelength (350 nm for these experiments) and the emission wavelength of the “planar” excited state was ascribed to fast vibrational relaxation of the excited molecule. The argument to explain the fluorescence dynamics in terms of a twisting motion lay in its strong solvent viscosity dependence. Recently, evidence for the twisted nature of the long-lived excited state was obtained from its resonance Raman spectrum.¹⁴

On the basis of the temperature-dependent behavior of the fluorescence,¹³ it was concluded that the twisting motion in TPE does not involve any intramolecular barrier. However, if we compare with the barrierless isomerizations mentioned above, we find that the conjectured rate of the isomerization process in TPE is 2 orders of magnitude slower. The discrepancy was explained by assuming that the twisting process is slowed considerably by collisions with the solvent molecules.

The excited state motion of TPE has also been studied through its $S_n \leftarrow S_1$ absorption spectra.¹⁵ Two transient absorption bands were observed: one at 450 nm, which is not influenced by the excited state motion, and another one at 600 nm, which disappears with the same time constant as the short-lived fluorescence. Therefore, the 600 nm absorption band was assigned to the “planar” excited TPE as well.

From theoretical considerations,¹⁰ it was predicted that a state with a large dipole moment can be formed after the twist of the

* Abstract published in *Advance ACS Abstracts*, May 1, 1995.

ethylenic bond, through the following mechanism. At the perpendicular conformation of the ethylenic bond, which is the most stable conformation after π, π^* excitation, mixing with a higher excited state occurs. This gives rise to two new states that are each other's mirror image; in each of these, one of the ethylenic p orbitals is empty and the other one contains both electrons. The large dipole moment can only be realized if the symmetry of the molecule is broken, because the two mirror-image states are fully degenerate in the symmetrical molecule and mix to form a nonpolar state. If symmetry is broken, one of the states is lowered in energy, and the other one is raised. Then, an electron will be transferred from one half of the molecule to the other half, so that the lowest-energy state is formed. In the following, we will refer to this state as the charge-separated (cs) state.

A similar phenomenon occurs in the excited state of another symmetric molecule, 9,9'-bianthryl.¹⁶ Measurements on 9,9'-bianthryl in small clusters have shown¹⁷ that charge separation is induced by asymmetry in the environment of the excited molecule, presumably of electrostatic character. Once symmetry is broken, a further stabilization can be expected because the dipole of the molecule in its cs state acts to increase asymmetry. Polar solvent molecules will orient themselves with respect to this dipole, thus increasing the electrostatic asymmetry in the environment of the solute.

Ab initio calculations on charge separation in ethylene¹⁸ have pointed out the role of pyramidalization around the electron-accepting ethylenic carbon atom in stabilizing the cs state. Here, one of the states is lowered in energy when the molecule is asymmetric with respect to this pyramidalization, i.e., when one of the ethylene carbon atoms is pyramidalized at a larger angle than the other one. Also in this picture, the cs state acts to increase asymmetry once it is formed, because the extra electron on the acceptor moiety favors the pyramidalized configuration.¹⁸

Gradually, evidence for the existence of the cs state in TPE was obtained. Both the internal conversion kinetics^{19,20} and the picosecond optical calorimetry transients²¹ of TPE could be described by assuming a large dipole moment on the molecule in its excited state. Direct evidence for this large dipole moment was obtained recently by time-resolved microwave conductivity measurements.²² Therefore, the existence of the cs state is beyond any doubt.

In nonpolar solvents, it was found that the symmetry breaking that leads to the cs state is reversible. An equilibrium between polar and nonpolar species was observed,^{23,24} and the dipolar relaxation time of the cs state of TPE²² could only be explained realistically by assuming that the dipole continuously flips back and forth, on a time scale somewhere in the 10 ps range. The observation of dipole flipping means that the stabilization of the asymmetric conformation in nonpolar environments can only be on the order of kT .

In this paper, we report a femtosecond pump-probe study of the initial dynamics involved in the twisting motion and the breaking of symmetry in TPE. Our results show that the twisting motion in TPE is much faster than previously assumed and is accompanied by a buildup of a coherent oscillation. We propose a different assignment for the short- and long-lived fluorescence, as well as for the 600–650 nm absorption band. We will also discuss the implications of our findings with respect to symmetry breaking and charge separation.

2. Experimental Section

The femtosecond pump-probe experiments were performed with a setup similar to the one described previously,²⁵ with a few modifications.

The main difference is the amplifier system. For the experiments described in this paper, we used a system of two bow-tie amplifiers in series, amplifying the output of a CPM laser. The first amplifier is the six-pass bow-tie amplifier as described before, pumped with the 511 nm line of a copper-vapor laser (Oxford Lasers ACL35) operating at 9 kHz. The output of this amplifier is fed into a second, four-pass bow-tie amplifier, pumped by the 578 nm line of the same copper-vapor laser. Sulforhodamine 640 is used as the gain medium in both amplifiers. In the first amplifier, a saturable absorber (Malachite Green) is introduced between the fourth and fifth passes. In the second amplifier, no saturable absorber is present. The output of the entire amplifier system consists of a train of pulses at 9 kHz, with pulse duration of 60 fs and pulse energy approximately 15 μ J, centered at 620 nm.

The excitation beam at 310 nm, which is at the maximum of the TPE $S_1 \leftarrow S_0$ absorption band, was generated by second harmonic generation in a 300 μ m thick KDP crystal. The probe beam was obtained by continuum generation in a 2 mm thick sapphire plate. Spectral parts of the continuum were selected by placing interference filters in front of the detector. To compensate for the chirp in the continuum, a double-pass grating pair was placed in the continuum beam. In this setup, the widths of the cross-correlations between pump and probe beams (measured by difference-frequency generation in a 300 μ m KDP crystal) are 90–130 fs for probe wavelengths in the entire spectral range from 400 to 700 nm. For all the reported experiments, the relative polarizations of pump and probe are at the magic angle.

The pump-induced absorption signals thus measured are so large (up to 15%) that a simple linear relation between measured signal and absorbance does not hold. All reported data are corrected for this and displayed on the absorbance scale.

Before use, the solid tetraphenylethylene was recrystallized at least twice from chloroform. The solvents ethanol and cyclohexane (Merck, p.a.) and 1-octanol and *n*-hexadecane (Janssen) were used as received. The experiments were performed on a 0.3 mm thick free flowing jet of a 2×10^{-3} M solution of TPE in one of the mentioned solvents. We used a fairly large amount of solution (500 mL) to avoid accumulation of any photoproducts.

3. Results

3.1. Subpicosecond Pump-Probe Delays. Qualitatively, the transients in all studied solvents look the same. Immediately upon excitation at 310 nm, two $S_n \leftarrow S_1$ absorption bands are found to grow in instantaneously: the 400–450 nm absorption band as reported by Greene¹⁵ and a broad absorption band, extending from 550 to 650 nm. The latter narrows and shifts to the red within a few hundred femtoseconds, thus forming the 600–650 nm band as reported by Greene.¹⁵ The spectral dynamics in the region from 500 to 650 nm at early times are displayed in Figure 1; as an example, the data for the ethanol solution are shown. The time constant associated with this spectral change was determined by fitting to a falling exponential at 550 nm and to a sum of an instantaneous component and a rising exponential at 650 nm; convolution with the relevant pump-probe cross-correlation was included in the fitting procedure. Both exponentials could, within error margins, be related to a single time constant, namely 220 ± 30 fs.

A modulation with a period of 270 fs (corresponding to a vibration frequency of 120 cm^{-1}) is observed in the 600–650 nm absorption band, most clearly at 650 nm. The modulation is damped out within a few oscillation periods. The oscillation is observed only in the 600–650 nm absorption band, in all

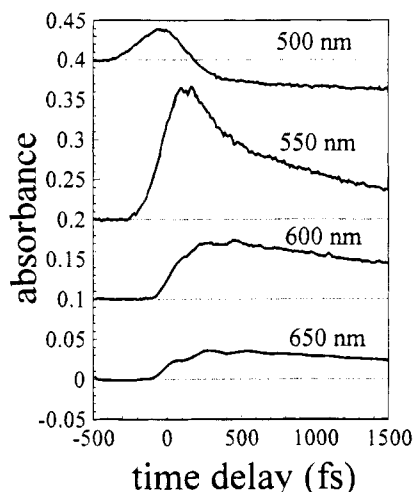


Figure 1. Short-time behavior of the excited-state absorption of TPE in ethanol, observed at four different probe wavelengths, as indicated in the figure. For reasons of clarity, the data for 600, 550, and 500 nm have been shifted vertically by 0.1, 0.2, and 0.4, respectively.

the studied solvents. The oscillation starts around time delay zero, with no apparent phase delay.

In order to examine the dynamics of the oscillations separately, the rising exponential as discussed in the first paragraph was subtracted, as well as a falling exponential to account for the dynamics of the absorption band on the picosecond time scale, which will be discussed in the next section. The result is shown in Figure 2. It is clear that the maximum amplitude of the oscillation does not occur at time zero, but somewhere around 200 ± 100 fs. This finding is not sensitive to the details of the model used to subtract the other contributions to the signal, nor is it dependent on the value of the time constant of the rising exponential. The negative oscillation before zero time delay is due to the fact that the steep rising flank was not described exactly by our model, and we do not attribute any physical significance to it. The measured buildup can be described by a time constant, which is within error margins the same as the one associated with the large spectral shift. It is even more clearly visible when we compare the measured transient to a simulation, assuming instantaneous excitation, convoluted with the pump-probe cross-correlation. This is the dashed line in Figure 2.

The time constant for the decay of the oscillations was determined from the width of the Fourier transform to be about 350 fs in ethanol and cyclohexane. For 1-octanol and *n*-hexadecane, we could not determine a value this way, but we can estimate from the smaller amplitude of the second recurrence that the decay rate there is higher than in ethanol and cyclohexane: roughly 250–300 fs, showing that the coherence decay is affected by solvent viscosity.

At 500 nm, we measure “negative absorbance” signals from 250 fs onward. Because the sample solutions do not exhibit any absorption at 500 nm when in equilibrium, these signals cannot be ascribed to bleaches, but must be attributed to $S_1 \rightarrow S_0$ stimulated emission. It is remarkable that stimulated emission is observed there so early already, because of the immense difference between the excitation and emission frequencies: as much as $12\,000\text{ cm}^{-1}$.

3.2. Longer Time Scales. When we look at longer pump-probe delays, up to 30 ps, we observe the following. The 600–650 nm absorption band loses intensity in 3–10 ps, dependent on solvent polarity and viscosity (see Figure 3). The absorption disappears completely in ethanol solution. In the other solvents, there is a long lived component of $\sim 25\%$ of the initial signal.

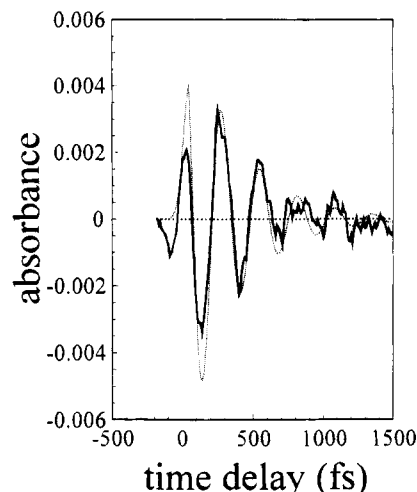


Figure 2. Oscillatory component of the 650 nm transient, separated from the other contributions to the transient as described in section 3.1, with a period of approximately 270 fs. The dashed line is a transient expected if there had not been a finite buildup time, calculated as described in section 3.1, showing a clear deviation from the experimental transient at shorter time delays.

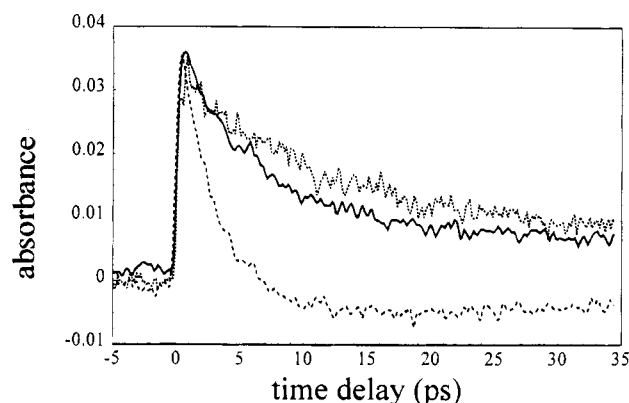


Figure 3. Decay of the excited-state absorption of TPE in three different solvents, observed when probing at 650 nm: solid line, cyclohexane; dashed line, ethanol; dotted line, *n*-hexadecane. The corresponding decay constants are tabulated in Table 1.

TABLE 1: Decay Times τ of the 600–650 nm Absorption Band of S_1 TPE

solvent	τ/ps
ethanol	2.8
1-octanol	9.6
cyclohexane	6.7
<i>n</i> -hexadecane	12.0

The transients could be described well by a single-exponential decay and a stationary background; the time constants of the exponential decays for the various solvents are tabulated in Table 1.

At 500 and 550 nm, as displayed in Figure 4, we observe a further red shift of the stimulated emission over an additional 2000 cm^{-1} , taking place in ~ 10 ps, as seen before by Barbara *et al.* using a time-resolved fluorescence detection apparatus.¹³

The 400–450 nm absorption band does not show any dynamics on time scales from 100 fs to 20 ps. At 450 nm, we see some changes at early times, which are due to the blue flank of the stimulated emission band growing in rapidly and shifting to the red on a somewhat longer time scale. At longer times, the absorption band slowly loses intensity; our data here are in accordance with the findings of Schilling and Hilinski.¹⁹ We infer from our observations that the 400–450 nm absorption band is hardly influenced by either twisting dynamics or

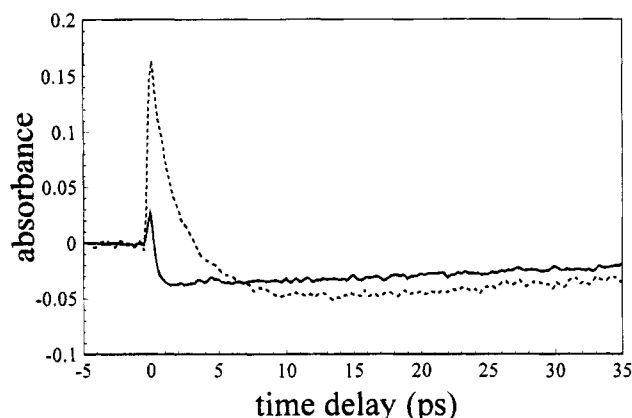


Figure 4. Pump-probe transients of TPE in ethanol, measured at probe wavelengths of 500 nm (solid line) and 550 nm (dashed line), at longer pump-probe delays. Negative signals denote stimulated emission. The red shift of the emission spectrum in time can be inferred from the fact that the maximum signal at 550 nm is reached later than at 500 nm.

coherent vibrations, which agrees with previous assignments.¹⁵ It is probably due to a π, π^* -like excitation localized on the phenyl rings, and we will not discuss it any further.

4. Discussion

4.1. Isomerization Dynamics. Our observations on the subpicosecond time scale indicate that large changes take place in the molecule in the first 250 fs. We observe two phenomena, occurring on this time scale: (1) a large change in the excited-state absorption spectrum and (2) the rise of stimulated emission, shifted as much as $12\,000\text{ cm}^{-1}$ to the red of the excitation frequency. These observations can be explained naturally in terms of an excited-state 90° twist, taking place on a time scale of about 250 fs. In particular, the second observation is irreconcilable with the previous picture of the excited-state dynamics of TPE, where fluorescence living for 5–15 ps was attributed to a “planar”, vibrationally relaxed excited state. Because of the time resolution of our experiments, we can now unambiguously say that the enormous red shift in emission only takes 250 fs, which can by no means be explained in terms of vibrational relaxation because it is so large and takes place so quickly. Therefore, we conclude that the excited molecule moves along the ethylenic twisting coordinate to a new geometry within a few hundred femtoseconds, instead of the previously assumed several picoseconds.

The rate of excited-state isomerization that follows from our interpretation is in good agreement with the rate measured for the barrierless isomerization reactions mentioned in the introduction: *cis*-stilbene¹¹ and the visual pigment rhodopsin.¹² Apparently, contrary to what has been suggested before,¹³ solvent viscous drag is not so important in the initial twisting motion. Nevertheless, we do see a marked viscosity dependence at longer time scales. This must be associated with the full geometric relaxation of the molecule. Because the ethylenic twist is so fast, the phenyl rings are initially lagging behind. In this conformation, there is a large strain on the phenyl carbon atoms that are directly attached to the ethylenic carbon, and this strain will be the driving force for the phenyl rings to assume their new equilibrium positions. Because of their bulkiness and the fact that they point outward from the molecule, equilibration is hindered by collisions with the environment. This geometric equilibration takes place in 5–10 ps, causing the further red shift of the emission in this time period.

4.2. Coherent Motion. We now turn to a discussion of the observed periodic modulations. First of all, we can rule out

the possibility that these modulations are due to coherent vibrations in the ground state, excited by an impulsive stimulated Raman process. The probing wavelengths in the red part of the spectrum are too far away from the ground-state absorption spectrum of TPE. Therefore, the modulation of the signal must be due to an excited-state vibration.

Because the oscillations are at all times more intense at the red edge of the band, the oscillations are most likely due to a modulation of the position of the absorption band. We have not observed any counterphase modulations on the blue edge of the absorption spectrum, as seen for the photoproducts of I_3^- ⁴ and rhodopsin,⁶ but this may be due to the fact that they are less intense there and overwhelmed by the stimulated emission signal and by the intense blue absorption.

The overall behavior of the 650 nm signal in the first few hundred femtoseconds consists of a small decrease after the first peak, followed by a much stronger increase due to the large red shift as discussed in the previous section. This behavior cannot be explained in terms of a one-dimensional picture, where only a recurrence of the wave packet can occur. We therefore conclude that the reaction process has to be described using at least a two-dimensional surface. This is different from the situation in rhodopsin, where isomerization and coherent motion were explained in a one-dimensional picture.⁶

As stated, the oscillation at 600 and 650 nm is not at its maximum around time zero, but after a definite buildup time, which corresponds well to the time associated with the twisting of the ethylenic bond. This is normally not what one would expect for a vibration that is excited at time zero and not coupled to the reaction coordinate. The situation at 650 nm is as follows: the probe frequency is originally on the red band edge, but after the shift it will be much closer to the band center. In general, oscillations due to vibrational coherence are most intense at the flanks of the absorption band,⁴ and therefore the modulations at 650 nm are expected to *decrease* in time while the red shift takes place.

The observation of an increase in modulation amplitude can be explained by a model in which vibrational coherence is *promoted* by the reactional motion. In this model, coherent vibrational motion is not excited directly in the optical excitation, but it is initiated by a coupling between motion along the twisting coordinate and the “oscillation coordinate”.

To gain more insight into the molecular dynamics, we have to find out which vibrational mode is excited coherently. The very low frequency of the oscillation ($\sim 120\text{ cm}^{-1}$), which is low even for a bending vibration, suggests that it is a motion in which large parts of the molecule are involved. When we compare our value with the assignments for the low-frequency vibrations in the stilbenes²⁶ and in 1,1-diphenylethylene,²⁷ we find that the most likely candidate is a torsional and/or scissoring motion of the phenyl rings, in other words: the torsion of the C(e)–C(Ph) bonds (where e stands for ethylene and Ph for phenyl), probably accompanied by a widening of the C(Ph)–C(e)–C(Ph') bond angle. The driving force to excite this motion will be the tendency of the unpaired electrons, that are created on the ethylenic carbons upon excitation,¹⁰ to delocalize over the phenyl rings, also observed in the radicals triphenylmethyl²⁸ and diphenylaminyl.²⁹ It requires that the phenyl rings are as much as possible in the C(Ph)–C(e)–C(Ph') plane, which they are not in the ground state conformation of TPE,³⁰ largely because of steric interactions between *cis*-positioned phenyl rings (see the schematic drawing in Figure 5). When moving into this plane, steric interactions with their neighbors attached to the same C(e) become important; this is the reason for our assumption that the scissoring motion has to be involved as well.

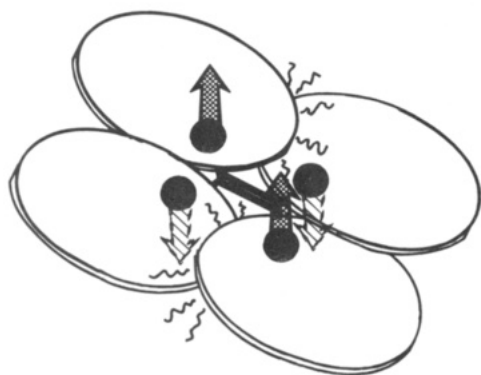


Figure 5. Schematic drawing of the TPE molecule to clarify the femto- and picosecond processes after excitation. In the ground state, the phenyl rings cannot lie in the ethylene plane, because they are in each other's way. The wavy lines indicate where steric interaction is strongest. When the 90° twist around the ethylenic bond takes place, the phenyl rings are dragged away from each other in 250 fs along the arrows, which largely reduces the steric strain near the wavy lines. The "far ends" of the phenyl rings are initially lagging behind; because of collisions with the surrounding solvent molecules, they take some picoseconds to reach their equilibrium positions.

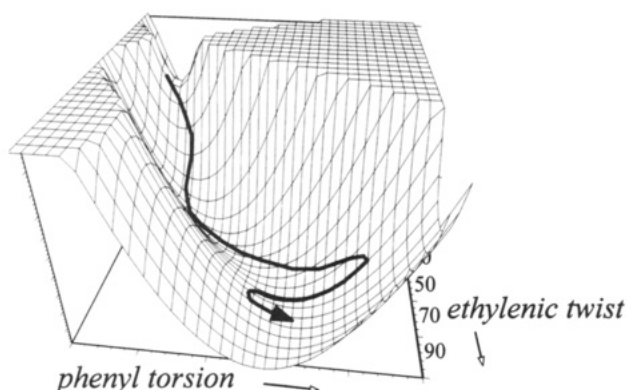


Figure 6. Sketch of the potential energy surface along the ethylenic twist, which is the major reaction coordinate, and the phenyl torsion, which is the coordinate along which coherent motion is excited in the twisting process. The heavy line is a sketch of a typical trajectory that the center of the wave packet will perform after excitation.

We can now construct a physical picture behind the impulsive excitation of the vibration. Initially, in the planar conformation, the rings are more or less locked to their position because of steric strain.³⁰ Steric interactions between phenyl rings that are originally on the *cis*-positions relative to each other disappear when the ethylene bond is twisted, as can be seen in the schematic drawing in Figure 5. The rings are relieved of this strain by the rapid twist and start to move in a concerted fashion. Collisions with the surrounding solvent molecules make the oscillations decay rapidly, which explains the observed solvent viscosity dependence of the coherence decay.

The mechanism of impulsive vibrational excitation can be described as follows. First, there is a rapid slide downhill along a barrierless coordinate, in the case of TPE: the twist of the ethylenic bond. This motion changes the equilibrium geometry along another coordinate, which is in the present case that of the phenyl torsion/scissoring mode. A qualitative picture of the potential surface associated with these motions is given in Figure 6. If motion along the first, barrierless coordinate takes place on the same time scale or faster than the oscillation period associated with the second coordinate, a wave packet starts to perform a periodic motion in this second coordinate around the new equilibrium position.

Viewed like this, the situation is much more analogous to the coherent excitation of product vibrations as observed in the

photodissociations of HgI_2 ,^{3,5} and I_3^- ⁴ than to the excitation mechanism as described for the rhodopsin chromophore.⁶ In spite of the similarities between the systems, also from a theoretical point of view,^{10,31} there are large differences when it comes to vibrational coherence associated with the reaction processes. This is even more pronounced when we compare rhodopsin and TPE with another member of the same class of reactive systems, *cis*-stilbene, where no vibrational coherence was observed at all. Apparently, there are many factors that determine whether and where coherent product vibrations can be observed. From the observed cases of vibrational coherence after ethylenic twist, it seems that some sort of strained environment is necessary, in which the twisted double bond poses a large, nearly instantaneous distortion. However, there are too few systems studied yet to draw a firm conclusion now.

4.3. Formation of the Charge-Separated (cs) State. So far, we have not said anything about the implications of our findings to the formation of the cs state. In fact, our observations indicate that there is no charge separation during the initial stage of the excited-state dynamics. When comparing the short-time results for the investigated solvents, we find that they are not so very much different. If charge separation occurred immediately upon excitation or immediately after the twist, one would expect large differences between the subpicosecond behavior in polar solvents, such as ethanol, and nonpolar solvents, such as cyclohexane, but this is not the case.

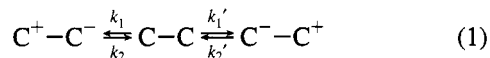
On the picosecond time scale, we do see a clear polarity dependence, namely, in the decay dynamics of the 600–650 nm absorption band (see Figure 3 and Table 1). Because of this observation, we ascribe the disappearing of this band to the charge transfer taking place. From the observed difference in the time constants found for the cyclohexane and *n*-hexadecane solvents, it is clear that the charge-transfer process is also affected by viscosity. Hence, charge transfer must be assisted by the picosecond geometric relaxation mentioned in the previous section. As expected from theory,¹⁸ the position of the phenyl rings around the ethylenic carbon atoms is very important for the stabilization or destabilization of the cs state with respect to the nonpolar state. This explains the connection between the formation of the cs state and the picosecond red shift of the $S_1 \rightarrow S_0$ stimulated emission, which we interpreted in terms of the geometric relaxation of the phenyl rings.

This picture also provides a mechanism for symmetry breaking. Both halves of the molecule, though indistinguishable, will not always be in identical conformations during the relaxation process. It will inevitably occur at one time or other that one of the diphenylmethyl moieties is in a more favorable conformation to accept the extra electron. This is caused by asymmetry in the collisions with the solvent molecules that hinder the relaxation process. This picture provides a second mechanism, next to the electrostatic one,¹⁷ in which asymmetry in the environment influences charge separation. It will be most important for nonpolar solvents, where electrostatic interactions are weak.

In most of the solvents studied, the red absorption does not disappear completely, but a long-lived absorption at 600–650 nm remains. This fact is in accordance with the observations of Greene and Scott²³ and Ma and Zimmt.²⁴ Both research groups found a long-lived remaining signal that they could attribute to the nonpolar species. They explained this by assuming that an equilibrium is established between the nonpolar (red-absorbing) and the cs (not red-absorbing) species. Our finding that there is no long-lived red absorption in ethanol solution supports this explanation. In a polar solvent, the solvent molecules will orient themselves with respect to the solute

dipole, thus stabilizing the cs state and shifting the equilibrium further away from the nonpolar state.

In the nonpolar solvents, this electrostatic stabilization is absent; we see a steady-state concentration of nonpolar excited TPE in equilibrium with the cs state. From this observation, we can estimate the rates associated with dipole flipping in nonpolar environments. Let us assume that the nonpolar state is a necessary intermediate state in the flip of the cs dipole. Then, the following simple kinetic scheme applies:



where $k_n = k_n'$ ($n = 1, 2$) averaged over the ensemble. From our data, we can obtain a reasonable estimate for $k_1 + k_1'$ from the decay time constant τ of the 600–650 nm absorption band, through $k_1 + k_1' = \tau^{-1}$. For the cyclohexane solution, this gives us $k_1 + k_1' = 1.5 \times 10^{11} \text{ s}^{-1}$. Furthermore, we can derive

$$\frac{k_1 + k_1'}{k_2 + k_2'} = \frac{P(C^+-C^-) + P(C^--C^+)}{P(C-C)} \quad (2)$$

where $P(X)$ denotes the concentration of species X. Since, for the cyclohexane solution, $P(C-C)$ after equilibration equals 0.25 times the total excited population, we can calculate that the ratio in eq 2 is equal to 3, giving a value for $k_2 + k_2' = 5 \times 10^{10} \text{ s}^{-1}$, corresponding to a time constant of 20 ps. For the *n*-hexadecane solution, we can perform the same calculation, leading to a rate of $k_2 + k_2' = 2.5 \times 10^{10} \text{ s}^{-1}$ there, which corresponds to 40 ps.

This calculation shows that the flipping of the dipole in nonpolar environments indeed takes place on a time scale of tens of picoseconds.²² We find that the rates associated with dipole flipping are affected by viscosity as well, indicating the importance of the phenyl motions for the dipole flipping process.

5. Conclusions

Our findings on the excited-state dynamics of TPE in the femtosecond time domain have shed new light on the excited-state twisting and charge separation processes in this molecule. We have found that the twist of the ethylenic bond only takes 250 fs, instead of the previously assumed 5–15 ps. This rapid twist reduces steric strain in the molecule, giving rise to a coherent scissoring or torsional motion of the phenyl rings, visible through a periodic modulation of the excited-state absorption. This mechanism for the buildup of a coherent oscillation is similar to the impulsive excitation of product vibrations by the very fast dissociations of HgI_2 and I_3^- . Further experiments, for instance time-resolved excited-state resonance Raman scattering, may shed more light on the nature of this excitation process.

Charge separation is a slower process and takes 3–10 ps, dependent on solvent polarity and viscosity. Its viscosity dependence shows that the bending motions of the phenyl rings around the ethylenic carbons play an important role in determining charge separation and dipole flipping dynamics. Asymmetries in these bending motions, caused by asymmetric collisions with the environment, determine which way the dipole of the cs state points.

Acknowledgment. We thank R. W. J. Zijlstra (Department of Organic and Molecular Inorganic Chemistry) for helpful discussions on the theoretical aspects of the charge separation process. We thank one of the referees for his instructive

criticism, inspiring us to look more deeply into the mechanism of the coherent oscillation. The investigations were supported by the Netherlands Foundations for Chemical Research (SON) and Physical Research (FOM) with financial aid from the Netherlands Organisation for the Advancement of Science (NWO).

References and Notes

- (1) Zewail, A. H. *J. Phys. Chem.* **1993**, *97*, 12427–12446. *Femtosecond Reaction Dynamics*; Wiersma, D. A., Ed.; North-Holland: Amsterdam, 1994. *Femtosecond Chemistry*; Manz, J., Wöste, L., Eds.; VCH Publishers: New York, 1994.
- (2) Rose, T. S.; Rosker, M. J.; Zewail, A. H. *J. Chem. Phys.* **1989**, *91*, 7415–7436.
- (3) Metiu, H.; Engel, V. *J. Opt. Soc. Am. B* **1990**, *7*, 1709–1726.
- (4) Dantus, M.; Bowman, R. M.; Gruebele, M.; Zewail, A. H. *J. Chem. Phys.* **1989**, *91*, 7437–7450.
- (5) Banin, U.; Waldman, A.; Ruhman, S. *J. Chem. Phys.* **1992**, *96*, 2416–2419.
- (6) Banin, U.; Ruhman, S. *J. Chem. Phys.* **1993**, *98*, 4391–4403.
- (7) Pugliano, N.; Palit, D. K.; Szarka, A. Z.; Hochstrasser, R. M. *J. Chem. Phys.* **1993**, *99*, 7273–7276.
- (8) Wang, Q.; Schoenlein, R. W.; Peteanu, L. A.; Mathies, R. A.; Shank, C. V. *Science* **1994**, *266*, 422–424.
- (9) Vos, M. H.; Lambry, J. C.; Robles, S. J.; Youvan, D. C.; Breton, J.; Martin, J. L. *Proc. Natl. Acad. Sci. U.S.A.* **1991**, *88*, 8885–8889.
- (10) Engel, V.; Metiu, H. *J. Chem. Phys.* **1991**, *95*, 3444–3455.
- (11) Jean, J. M.; Fleming, G. R.; Friesner, R. A. *Ber. Bunsen-Ges. Phys. Chem.* **1991**, *95*, 253–258.
- (12) Ben-Nun, M.; Levine, R. D. *Chem. Phys. Lett.* **1993**, *203*, 450–456.
- (13) Saltiel, J. *J. Am. Chem. Soc.* **1967**, *89*, 1036–1037.
- (14) Saltiel, J.; Zafiriou, O. C.; Megarity, E. D.; Lamola, A. A. *J. Am. Chem. Soc.* **1968**, *90*, 4759–4760.
- (15) Bonačić-Koutecký, V.; Bruckmann, P.; Hiberty, P.; Koutecký, J.; Leforestier, C.; Salem, L. *Angew. Chem., Int. Ed. Engl.* **1975**, *14*, 575–576.
- (16) Salem, L. *Science* **1976**, *191*, 822–830.
- (17) Bonačić-Koutecký, V.; Koutecký, J.; Michl, J. *Angew. Chem., Int. Ed. Engl.* **1987**, *26*, 170–189.
- (18) Abrash, S.; Repinec, S.; Hochstrasser, R. M. *J. Chem. Phys.* **1990**, *93*, 1041–1053.
- (19) Todd, D. C.; Jean, J. M.; Rosenthal, S. J.; Ruggiero, A. J.; Yang, D.; Fleming, G. R. *J. Chem. Phys.* **1990**, *93*, 8658–8668.
- (20) Rice, J. K.; Baranavski, A. P. *J. Phys. Chem.* **1992**, *96*, 3359–3366.
- (21) Schoenlein, R. W.; Peteanu, L. A.; Mathies, R. A.; Shank, C. V. *Science* **1991**, *254*, 412–415.
- (22) Peteanu, L. A.; Schoenlein, R. W.; Wang, Q.; Mathies, R. A.; Shank, C. V. *Proc. Natl. Acad. Sci. U.S.A.* **1993**, *90*, 11762–11766.
- (23) Schoenlein, R. W.; Peteanu, L. A.; Wang, Q.; Mathies, R. A.; Shank, C. V. *J. Phys. Chem.* **1993**, *97*, 12087–12092.
- (24) Barbara, P. F.; Rand, S. D.; Rentzepis, P. M. *J. Am. Chem. Soc.* **1981**, *103*, 2156–2162.
- (25) Tahara, T.; Hamaguchi, H. *Chem. Phys. Lett.* **1994**, *217*, 369–374.
- (26) Greene, B. I. *Chem. Phys. Lett.* **1981**, *79*, 51–53.
- (27) Schneider, F.; Lippert, E. *Ber. Bunsen-Ges. Phys. Chem.* **1968**, *72*, 1155–1160.
- (28) Kahlow, M. A.; Kang, T. J.; Barbara, P. F. *J. Phys. Chem.* **1987**, *91*, 6452–6455.
- (29) Mataga, N.; Yao, H.; Okada, T.; Rettig, W. *J. Phys. Chem.* **1989**, *93*, 3383–3386.
- (30) Honma, K.; Kajimoto, O. *J. Chem. Phys.* **1994**, *101*, 1752–1754.
- (31) Buenker, R. J.; Bonačić-Koutecký, V.; Pogliani, L. *J. Chem. Phys.* **1980**, *73*, 1836–1849.
- (32) Schilling, C. L.; Hilinski, E. F. *J. Am. Chem. Soc.* **1988**, *110*, 2296–2298.
- (33) Sun, Y. P.; Fox, M. A. *J. Am. Chem. Soc.* **1993**, *115*, 747–750.
- (34) Sun, Y. P.; Bunker, C. E. *J. Am. Chem. Soc.* **1994**, *116*, 2430–2433.
- (35) Morais, J.; Ma, J.; Zimmt, M. B. *J. Phys. Chem.* **1991**, *95*, 3885–3888.
- (36) Schuddeboom, W.; Jonker, S. A.; Warman, J. M.; de Haas, M. P.; Vermeulen, M. J. W.; Jager, W. F.; de Lange, B.; Feringa, B. L.; Fessenden, R. W. *J. Am. Chem. Soc.* **1993**, *115*, 3286–3290.
- (37) Greene, B. I.; Scott, T. W. *Chem. Phys. Lett.* **1984**, *106*, 399–402.
- (38) Ma, J.; Zimmt, M. B. *J. Am. Chem. Soc.* **1992**, *114*, 9723–9724.
- (39) Lenderink, E.; Duppen, K.; Wiersma, D. A. *Chem. Phys. Lett.* **1992**, *194*, 403–409.
- (40) Warshel, A. *J. Chem. Phys.* **1975**, *62*, 214–221.
- (41) Meić, Z.; Güsten, H. *Spectrochim. Acta* **1978**, *34A*, 101–111.
- (42) Bree, A.; Zwarich, R. *J. Mol. Struct.* **1981**, *75*, 213–224.
- (43) Judeikis, H.; Kivelson, D. *J. Am. Chem. Soc.* **1962**, *84*, 1132–1134.
- (44) Neugebauer, A.; Bamberger, S. *Chem. Ber.* **1974**, *107*, 2362–2382.
- (45) Hoekstra, A.; Vos, A. *Acta Crystallogr. B* **1975**, *31*, 1716–1721.
- (46) Salem, L.; Bruckmann, P. *Nature* **1975**, *258*, 526–528.